Tervalent Conducting Polymers with Tailor-Made Work Functions: Preparation, Characterization, and Applications as Cathodes in Electroluminescent Devices

Corey J. Bloom, C. Michael Elliott,* Paul G. Schroeder, C. Brian France, and Bruce A. Parkinson

Contribution from the Department of Chemistry, Colorado State University, Fort Collins, Colorado 80523

Received May 31, 2001

Abstract: A series of conducting polymers have been prepared through thermal polymerization of transition-metal diimine complexes. The as-polymerized material is electrochemically converted into its formally zerovalent form. Due to the proximity of the half-wave potentials of the formal 1+/0 and 0/1− couples, there is substantial disproportionation of the redox sites at room temperature, resulting in a conductive tervalent mixed-valent material. The redox processes that give rise to this mixed-valent material are predominantly ligand-based, and therefore are highly sensitive to substitution on the ligand periphery. Solution redox chemistry of the monomer can be used to accurately predict the work function of the corresponding zerovalent conducting polymer, which has been verified by ultraviolet photoelectron spectroscopy. Many of these materials have especially low work functions (<3.6 eV) making them appropriate materials to use as cathode materials in organic light-emitting devices (OLEDs). Working examples of tris(8-hydroxyquinoline)aluminum(III)-based OLEDs have been fabricated using one of these polymers as a cathode.

Introduction:

There has been increasing recent interest in light-emitting devices based on thin organic films of electroluminescent polymers or small molecules (organic light-emitting devices or OLEDs). Such systems offer several potential advantages over the more traditional inorganic light-emitting devices, including relative ease of production and processing.[1−3] While many different systems have been examined, all are essentially variations on a theme. Typically, these devices consist of one or more organic layers situated between a low work function metal cathode such as calcium and a higher work function anode, often transparent indium−tin oxide (ITO). When a sufficient potential bias is applied across the electrodes, electrons are injected from the cathode into the conduction band of the luminescent layer, and holes are injected from the anode into the valence band.[4] Under the influence of the applied potential, electrons and holes migrate to a plane within the organic film, where they meet. In an electroluminescent (EL) film, there is a reasonably high probability of photon emission due to electron−hole recombination. When this occurs, photons of an energy determined by the band gap (or HOMO/LUMO gap, as the case may be) are produced.

The number of charge carriers injected from the two electrodes is generally not equal. In this case, the current passed through the film will be determined by the majority carriers, while the emission of light will be limited by the minority carriers. Optimum emission efficiency is thus obtained when the rates of hole and electron injection are matched. The exact mechanism whereby charge injection occurs is a matter of some controversy and, indeed, may vary for different materials and device construction motifs. That point notwithstanding, there is at least an empirical relationship between the rates of charge carrier injection and the proximity of the Fermi level energies of the respective electrode to the energy of the band (or orbital) into which charge is injected. In other words, the Fermi energy of the anode should match the valence band energy, while the Fermi energy of the cathode should match the conduction band energy.

The simplest class of OLEDs are those composed of a single polymer layer between the two electrodes. The most commonly studied polymeric EL material of this type is an alkoxy-substituted poly-*p*-phenylene vinylene, generally referred to as MEH-PPV.[1−3,5−8] This polymer, which is soluble in organic solvents such as xylene, is typically spin-coated onto an ITO substrate, and a thin layer of calcium metal is then deposited on top to act as the cathode. For MEH-PPV, the work functions of both the ITO anode and Ca cathode match up very well to the respective bands in the polymer. In the case of the cathode, the work function of calcium is 2.9 eV, while the conduction band of MEH-PPV lies 2.8 eV below the vacuum level. Theoretically then, this junction should be very close to ideal

(1) Miyata, S.; Nalwa, H. S. *Organic Electroluminescent Materials and Devices*; Gordon and Breach: the Netherlands, 1997.

(2) Burroughs, J. H.; Bradley, D. D. C.; Brown, A. R.; Marks, R. N.; Mackay, K.; Friend, R. H.; Burns, P. L.; Holmes, A. B. *Nature* **1990**, *347*, 539−541.

(3) Gustafsson, G.; Cao, Y.; Treacy, G. M.; Klavetter, F.; Colaneri; Heeger, A. J. *Nature* **1992**, *357*, 472−479.

(4) *Depending on the specific type of material constituting the light emitting layer and the degree of orbital delocalization therein, it might be more appropriate to describe the injection of electrons and holes as being into LUMOs and HOMOs, respectively. Also, charge carrier injection might or might not be directly from the respective electrode into the bands of the luminescent layer, again depending on the construction of the particular device under consideration.*

(5) Reib, W. In *Organic Electroluminescent Materials and Devices*; Miyata, S., Nalwa, H. S., Eds.; Gordon and Breach: the Netherlands, 1997.

(6) Lazzaroni, R.; Bredas, J. L. *Plast. Eng.* **1998**, *43*, 185−197.

(7) Birgeson, J.; Fahlman, M.; Brohms, P.; Salaneck, W. R. *Synth. Met.* **1996**, *80*, 125−130.

(8) Parker, I. D. *J. Appl. Phys.* **1994**, *75*, 1656−1666.

in terms of the relevant energy match; however, studies have indicated several complications. Localized destructive heating,[2] oxide layer buildup, and calcium doping into the polymer[7] are a few experimentally proven examples.

An alternate approach in constructing OLEDs employs small-molecule organic compounds as EL materials in combination with one or more layers of charge-transport materials.[1,9–14] A common system uses tris(8-hydroxyquinoline) aluminum(III) complex (Alq_3) as both the EL and electron-transport material. Because Alq_3 does not efficiently conduct holes,[12,15] an additional "hole-transport material" layer is placed between the anode and the EL layer. These materials are usually triarylamine-based compounds such as *N,N*′-bis(3-methylphenyl)-*N,N*′-diphenylbenzidine (TPD). A typical literature device[12] would thus consist of layers as follows: ITO anode/TPD/Alq_3/metal cathode. As with the polymer-based devices, oxide buildup, degradation of the Alq_3, and other problems have been observed at the metal/organic interface.[11,13]

Given these documented problems, conducting polymers with equivalently low work functions might offer some significant advantages over metals as cathodes in these devices. First, a polymer–EL organic junction should be more compatible from a materials perspective. Second, impurities, oxides, or other degradation products would not necessarily be confined to the interface as they no doubt are with a metal contact. Finally, higher quantum efficiencies and longer lifetimes could result from increased stability imparted by such a junction.

Below we describe the preparation of three conducting polymers which, as we will show, have work functions that can be accurately predicted from the solution electrochemistry of the corresponding monomer and verified by UPS spectroscopy on the polymers. Our results indicate that, by making appropriate synthetic modifications to the monomer, it will be possible to "tune" polymer work functions in a predictable way. Finally, the work function of the specific polymers under consideration herein ranges from 3.7 to 3.0 eV. The lower end of this range matches the work function of some of the metals commonly used as cathodes in OLEDs. We have succeeded in using this lowest work function polymer to construct working devices based on Alq_3 as the electroluminescent film.

II. Experimental Section

Chemicals. Acetonitrile was Aldrich Optima grade, stored over 4 Å molecular sieves. THF from Aldrich was freshly distilled under N_2 from sodium and benzophenone. Ammonium hexafluorophosphate ($NH_4^+PF_6^-$) was purchased from Elf Atochem. Other electrolytes, tetra-*n*-butylammonium hexafluorophosphate ($TBA^+PF_6^-$) and poly(diallyldimethylammonium hexafluorophosphate), $PDDA^+PF_6^-$, were prepared as described elsewhere.[16] 4,4′-Dimethyl-2,2′-bipyridine (DMB) was obtained from Reilly Industries and was recrystallized from ethyl acetate and dried under vacuum at room temperature for 12 h prior to

Figure 1. Structure of monomer **M1**.

Figure 2. Structure of monomer **M2**.

use. The tris(8-hydroxyquinoline) aluminum(III) complex (Alq_3) was purchased from Aldrich and purified by sublimation at 350 °C and $P \approx 1 \times 10^{-3}$ Torr. *N,N*′-Bis(3-methylphenyl)-*N,N*′-diphenylbenzidine (TPD) also was purchased from Aldrich.

Synthesis of monomers M1 and M2 (Figures 1 and 2). Monomers M1 and M2 were synthesized as previously reported.[16,17]

Synthesis of monomer M3 (Figure 3): 4,4′-Bis-(5-bromo-pentyl)-2,2′-bipyridine (1). All glassware was dried in a 150 °C oven and cooled under N_2 flow. The reaction and all transfers were performed under N_2, and the reaction vessel was cooled with dry ice/acetone at all times. Thirty milliliters of dry THF was placed in a 1 L three-neck flask and cooled 30 min. Diisopropylamine (Aldrich) was filtered over neutral Al_2O_3 and purged with N_2 for 15 min. Diisopropylamine (7.80 mL, 0.056 mol) was syringed into THF and cooled. *n*-Butyllithium solution (28.0 mL, 2.0 M in cyclohexane, 0.056 mol) was slowly added via syringe and allowed to cool. DMB (5.01 g, 0.0273 mol) was dissolved in 350 mL of dry THF and placed in a 500 mL dropping funnel. The DMB solution was added dropwise over the course of 25 min, yielding a very dark red solution. After 2 h, 13.0 mL of 1,4-dibromobutane (Aldrich, N_2 purged for 15 min.) was added via syringe, following which the color slowly changed to turquoise. The reaction was cooled for 2 h more and left under N_2 to warm slowly to room temperature. After 12 h, 200 mL of deionized water was added to give

(9) Sheats, J. R.; Antoniadis, H.; Hueschen, M.; Leonard, W.; Miller, J.; Moon, R.; Roitman, D.; Stocking, A. *Science* **1996**, *273*, 884–888.

(10) Hamda, Y.; Sano, T.; Fujita, M.; Fujii, T.; Nishio, Y.; Shibata, K. *Jpn. J. Appl. Phys.* **1993**, *32*, L514–L515.

(11) Choung, V. E.; Mason, M. G.; Tang, C. W.; Gao, Y. *Appl. Phys. Lett.* **1998**, *72*, 2689–2691.

(12) Tang, C. W.; VanSlyke, S. A. *Appl. Phys. Lett.* **1987**, *51*, 913.

(13) Schlaf, R.; Schroder, P. G.; Nelson, M. W.; Parkinson, B. A.; Merritt, C. D.; Crisafulli, L. A.; Murata, H.; Kafafi, Z. H. *Surf. Sci.* **2000**, *450*, 142–152.

(14) Bulovic, V.; Tian, P.; Burrows, P. E.; Gokhale, M. R.; Forrest, S. R.; Thompson, M. E. *Appl. Phys. Lett.* **1997**, *70*, 2954–2956.

(15) Tang, C. W.; VanSlyke, S. A.; Chen, C. H. *J. Appl. Phys.* **1989**, *65*, 3610.

(16) Elliott, C. M.; Redepenning, J. G. *J. Electroanal. Chem.* **1986**, *197*, 219–232.
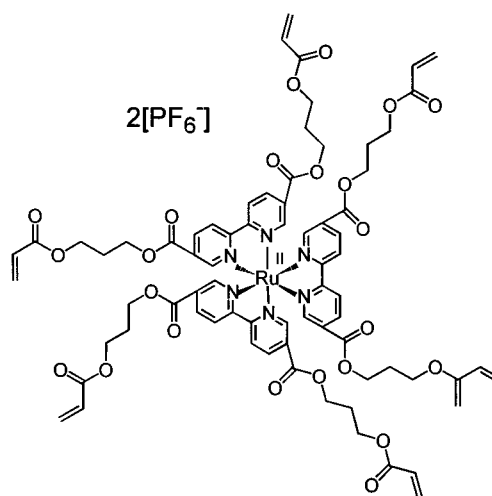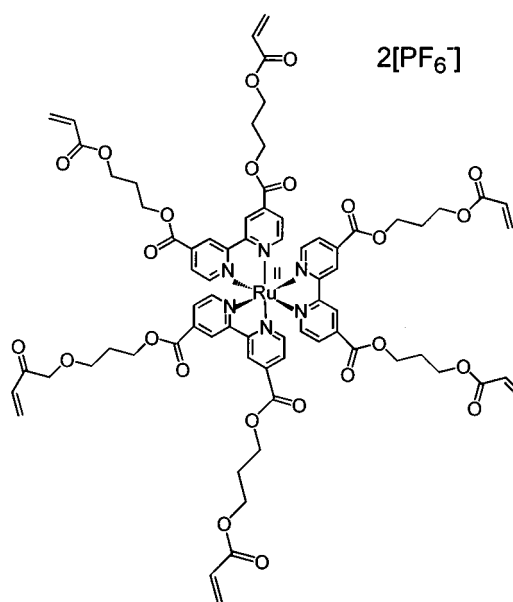
(17) Elliott, C. M.; Pichot, F.; Bloom, C. J.; Rider, L. S. *J. Am. Chem. Soc.* **1998**, *120*, 6781–6784.
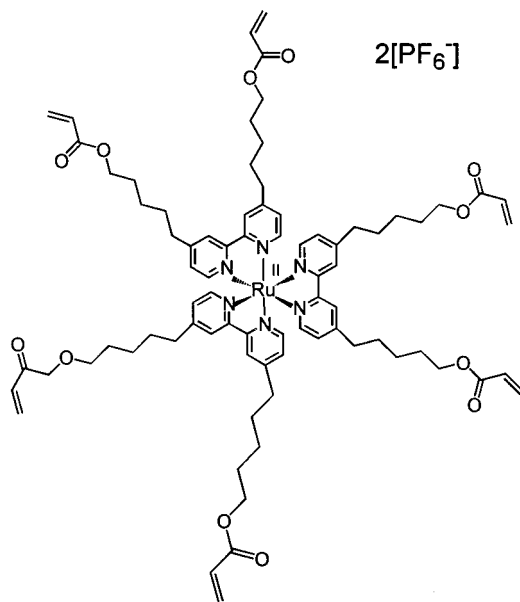
2[PF$_6^-$]

Figure 3. Structure of monomer **M3**.

a cloudy, slight yellow mixture. Volatile organics were removed by rotoevaporation, and the aqueous layer was extracted four times with equal volume CH$_2$Cl$_2$. Organic fractions were combined and dried over Na$_2$SO$_4$. The product **1** was purified by column chromatography with gradient CH$_2$Cl$_2$/acetone elution over flash silica gel.

Acetic acid 5-[4′-(5-acetoxy-pentyl)-2,2′-bipyridinyl-4-yl]-pentyl ester (2). **1** (500 mg) was added to a solution of 200 mg sodium acetate (Aldrich) in 30 mL glacial acetic acid (Mallinckrodt). The mixture was refluxed for 72 h under N$_2$ and neutralized to pH 6, at which time **2** precipitated out.

5-[4′-(5-Hydroxy-pentyl)-2,2′-bipyridinyl-4-yl]-pentan-1-ol (3). The crude product from the preparation of **2** was added to excess KOH in 250 mL of 95% ethanol. The solution was refluxed 12 h under N$_2$. Following neutralization with dilute acetic acid, ethanol was removed by rotoevaporation, and **3** precipitated out. The product was purified by column chromatography with gradient CH$_2$Cl$_2$/acetone elution over flash silica gel.

Acrylic Acid 5-[4′-(5-acryloyloxy-pentyl)-2,2′-bipyridinyl-4-yl]-pentyl Ester (4). **3** (300 mg) was placed in 200 mL of CH$_3$CN. Acryloyl chloride (8 mL, Aldrich) was added, and the solution refluxed for 6 h under N$_2$. After rotoevaporation of the solvent, a brownish sludge remained, smelling strongly of acryloyl chloride. Triethylamine (150 mL of a 2% aqueous solution) was added, and extracted four times with CH$_2$Cl$_2$. Fractions were combined, dried, and purified in the same manner as that for product **1**. Overall yield of a colorless, greasy solid approximately 10%. ^{1}H NMR in CD$_3$Cl (δ in ppm, multiplicity, integration) 1.4(p, 4H); 1.7(m, 8H); 2.7(t, 4H); 5.9(d of d, 2H); 6.2(m, 2H); 6.4(d of d, 2H); 7.2(d of d, 2H); 8.3(s, 2H); 8.6(d, 2H).

Tris-[acrylic Acid 5-[4′-(5-acryloyloxy-pentyl)-2,2′-bipyridinyl-4-yl]-pentyl ester]ruthenium(II) Hexaflourophosphate (M3). **4** (4 mol equiv, typically ∼150 mg) was dissolved in absolute ethanol (50 mL). Ru(DMSO)$_4$Cl$_2$ (1 mol equiv, ∼50 mg) was dissolved in 10 mL of deionized water. The light-yellow aqueous solution was added to the ligand solution, which quickly turned orange. The solution was refluxed 2 h under N$_2$. The solvent was rotoevaporated, and H$_2$O was added to 100 mL of total volume. Excess (∼400 mg) NH$_4^+$PF$_6^-$ was added, and an orange precipitate formed immediately. The solid was filtered, washed with water, and dissolved in CH$_3$CN. The solvent was evaporated to a small volume, and the complex was precipitated again by addition of diethyl ether. The product was again filtered, washed once with ether and twice with H$_2$O, redissolved in acetonitrile, and dried over Na$_2$SO$_4$. The product was purified by column chromatography over flash silica with gradient elution from 1:1 CH$_3$CN:H$_2$O to 50:49:1 CH$_3$CN:H$_2$O:saturated aqueous KNO$_3$. Yield of orange, oily solid approximately 70%. ^{1}H NMR in CD$_3$CN (δ in ppm, multiplicity, integration) 1.4(p, 4H); 1.7(m, 8H); 2.7(t, 4H); 5.9(d of d, 2H); 6.2(m, 2H); 6.4(d of d, 2H); 7.3(d, 2H); 7.7(m, 2H); 8.5(d, 2H).

Polymerization of Monomers. Thin films of **M1**, **M2**, or **M3** can be cast in a variety of ways and polymerized either thermally or photochemically, producing the corresponding respective polymers **P1**, **P2**, and **P3**. In all of the work discussed herein, polymerization was effected thermally at 150 °C. The exact polymerization conditions varied, depending on the film thickness and the substrate material, and whether the polymerization was carried out in air or under inert atmosphere, etc. Generally speaking, films reach the desired degree of polymerization more quickly in the absence of oxygen and more quickly on platinum than on ITO or glassy carbon. The addition of a radical initiator speeded the process but was not necessary and was not employed in the films discussed here. Films of the monomers and resulting polymers were flat, glassy, and appeared to be amorphous. Inspection visually, by optical microscope, and by scanning electron microscopy did not reveal any secondary structure.

Electrochemistry. Preparation of Materials for Determination of Fermi Level Energies. Monomer films approximately 400 nm thick (Sloan DekTak profilometer) were drop-coated from acetonitrile on a polished and cleaned glassy carbon electrode, polymerized approximately 6 h at 150 °C, and washed with CH$_3$CN. Cyclic voltammetry was performed in a Luggin capillary cell with Ag/Ag$^+$ 0.1 M in DMSO reference (+0.41 V vs NHE), Pt wire counter, and 0.1 M TBA$^+$PF$_6^-$ in acetonitrile electrolyte. Scan rates were 50 mV/sec or 100 mV/sec. Electronics consisted of P.A.R. model 173 Potentiostat and model 175 Programmer with output to Yokogawa X/Y recorder.

Electrochemistry. Preparation of Materials for UPS Spectroscopy. Thinner films of the monomer (approximately 100 nm) were drop-coated from CH$_3$CN on an ultrahigh vacuum (UHV) sample plate covered by Pt foil (previously flame-cleaned and sonicated in absolute ethanol) and polymerized for 2−3 h at 150 °C. Samples were then introduced into an inert atmosphere box and washed with CH$_3$CN. Alternately, the samples can be coated and polymerized entirely inside the box. Electrochemical reduction was done in a glass vial cell using the same reference electrode, counter electrode, and electronics as above. Polymeric electrolyte was PDDA$^+$PF$_6^-$ 0.05 M in acetonitrile. The polymer-coated working electrode (WE) was scanned only in the reductive direction at 2 mV/sec to approximately 300 mV past the second reduction wave (for example, **P3** film scanned to −2.1 V). The potential was held for 30−60 s before disconnecting the WE. Upon reduction, all three films exhibited modest but quite obvious color changes. Samples were washed three times in clean CH$_3$CN and placed behind the gate valve inside a UHV transfer rod. The gate valve was closed while still inside the glovebox and the entire transfer assembly removed.

UPS Studies. All UPS data were collected in an Omicron multiprobe UHV chamber (base pressure 5 × 10^{-11} Torr) equipped with a VSW EA125 single-channel analyzer. The transfer rod assembly was affixed to the entry chamber and pumped down to vacuum prior to introducing the samples into the analysis chamber. A helium lamp was used as the UV light source, providing a HeI line at 21.22 eV and a HeII line at 40.81 eV. A −5.00 V bias was applied to the samples to separate the sample and spectrometer high binding energy cutoffs. Kinetic energy analysis of electrons emitted normal to the sample was done using a 10 eV pass energy. The spectrometer was calibrated with an Ar$^+$ ion sputtered copper standard.

A straight line was fit on the secondary edge of the UPS HeI spectra. The intercept of this line with the abcissa determines the high binding energy cutoff (HBEC). A value of 0.1 eV was subtracted from the HBEC to correct for spectrum broadening due to thermal and analyzer effects.[13] The work function was determined by subtracting this value from the source energy of 21.22 eV.

OLED Construction. An acetonitrile solution of **M3** was spin-cast on a patterned ITO substrate. The homemade spin-caster consisted of an Oster variable-speed blender with a modified base peg such that flat substrates could be attached with double-stick tape. The lowest blender speed is 4000 rpm; to achieve slower rates a Variac was used. Films for devices were cast inside the glovebox at about 2000 rpm using this method. While still in the glovebox, films were polymerized for 3 h at 150 °C, rinsed, and electrochemically reduced. Samples were then placed inside the vacuum deposition chamber (Denton DV502A turbo model) which is directly interfaced to the box. At pressures below

6×10^{-6} Torr, the three materials were sequentially thermally deposited. The thicknesses of Alq_3 and TPD layers were approximately 450 Å, while the gold anode layer was about 800 Å, as measured by Leybold Inficon quartz crystal microbalance and XTM-2 Deposition Monitor. Device testing was done using the electrochemical instrumentation described above, with an added simple external circuit to provide $3\times$ multiplication of voltage output from the potentiostat. Light output was measured with a Hamamatsu photomultiplier tube driven at $400-800$ V.

III. Background and Theory

General Considerations. Under the conditions used to form polymers **P1**, **P2**, and **P3**, we estimate from earlier IR studies that, on average, approximately $1-1.5$ of the six total acrylate groups per monomer are consumed in the polymerization process—the remainder are unchanged.[18,19] At this level of cross-linking, the polymers swell in contact with most electrochemical solvents. Standard electrolyte ions (e.g., TMA^+ or PF_6^-) can freely move between the polymer and solution during electrochemical changes in oxidation state. The concentration of [Ru-$(LL)_3]^{2+}$ redox sites is estimated to be between 1.5 and 3.0 M. Spectral and electrochemical data show no indication of strong site−site interactions; consequently, it is assumed that the mechanism of electron transport through the polymer is by electron hopping from one localized site to another.

If consideration of a $[Ru(LL)_3]^n$-based polymer is limited to the formal Ru(III) and Ru(II) oxidation states, several generalizations can be made about its conductivity. When a $[Ru-(LL)_3]^n$ polymer is sandwiched between two metallic contacts, it will have measurable electronic conductivity only when mixed valent in the usual sense (i.e., when n is a noninteger). Furthermore, if the counterions present in the polymer are mobile, redox-state gradients will form under an applied potential.[20] Even when the counterions have limited local mobility, as in a dry film at low temperature, mixed-valent materials of this sort are still electronically conductive. In this case the oxidation-state gradients are simply prevented from forming.[21] Finally, since the metal-based redox couple is well separated from other redox processes in the polymer (by ≥ 2.4 V), the only necessary criterion for determining mixed valency is the value of n (i.e., whether it is 3, 2 or something in between).

When consideration is expanded to encompass other [Ru-$(LL)_3]^n$ oxidation states, the situation with regard to conductivity becomes more complex. When the difference between the apparent standard potentials for two redox processes approaches RT/nF, integer values of n can no longer be used to establish single valency. *Irrespective of the value of n, pure single oxidation states at the molecular level can no longer exist due to disproportionation.* The value of n thus reflects only the average charge per redox site and not the actual molecular-level site-valency. For **P1**−**P3**, the ligand-based redox potentials are such that these materials are significantly mixed-valent, and thus conductive, over the entire potential range spanning from the $2+/1+$ to the $3-/4-$ formal redox couples.

To more quantitatively expand the preceding discussion it is useful to consider a simplified system consisting of a hypothetical polymer having only two redox processes. For the sake of illustration these two redox processes will be assumed to involve $1+/0$ and $0/1-$ couples having a separation in formal potential,

(18) Sprinkle, R. B. Master's Thesis, Colorado State University, Fort Collins, CO, 1990.
(19) Bloom, C. J.; Elliott, C. M. Unpublished results.
(20) Jernigan, J. C.; Murray, R. W. *J. Phys. Chem.* **1987**, *91*, 2030−2032.
(21) Chidsey, C. E. D.; Murray, R. W. *J. Phys. Chem.* **1986**, *90*, 1479−1484.
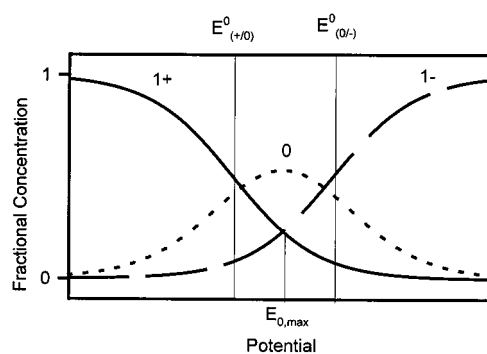
Figure 4. Fractional concentration vs potential for a mixed valence redox polymer with 140 mV separation between E_0's. Calculated at room temperature using the Nernst equation.

ΔE_0, of 0.140 V.

$$\Delta E_0 = E_0(1+/0) - E_0(0/1-) \tag{1}$$

Using the Nernst equation the redox composition of this polymer can be mapped as a function of potential. Figure 4 is a plot of the concentration of each oxidation state (normalized for the concentration of total redox sites in the polymer) versus potential. The potential axis lacks specific voltage values because it represents a generic example; however, the separation between the two E_0 corresponds to 0.140 V. Because we have restricted the system to three formal oxidation states, at potentials significantly more positive than $E_0(1+/0)$ or significantly more negative than $E_0(0/1-)$ the polymer would be essentially monovalent (either $1+$ or $1-$, respectively) and, therefore not electronically conductive. In contrast, when the applied potential is precisely midway between the two E_0's,

$$E_{(0,\text{max})} = [E_0(1+/0) + E_0(0/1-)]/2 \tag{2}$$

the net charge on the fixed redox sites is zero ($n = 0$); however, because of significant disproportionation, the material is mixed-valent and should be conductive.

Up to this point nothing considered has been unique to the case of $n = 0$. An otherwise identical polymer having any three formal oxidation states (m, $m-1$, and $m-2$) would produce exactly the same type of composition versus potential distribution as illustrated in Figure 4. The unique consequence of having $n = 0$ is that the polymer requires *no* physically mobile counterions to maintain charge balance. Since redox sites with $1+$ and $1-$ charges are mutually compensating, other counterions are not necessary. As a result, redox gradients are not possible because charge neutrality requires that $[1+] = [1-]$ at every point within the polymer. Electron-hopping conduction can still occur by electron exchange between $0/1+$ and $1-/0$ sites, but the redox composition must remain uniform throughout the polymer. Also, having no physically mobile counterions means that the polymer's composition cannot change due to ion migration or diffusion. With conventional mixed-valent polymers, ions can potentially be driven across the interface into another phase, resulting in a change in the redox composition of both phases. Assuming the second phase also contains no ions, there is no way to change the composition of the zerovalent polymer and still maintain electroneutrality.

Polymers formed from $[Ru(LL)_3]^{2+}X^-_2$ complexes have considerably more complex redox chemistry than the hypothetical example just discussed. Irrespective of that complexity, they all have (in common with the example polymer) stable and accessible $1+$, 0, and $1-$ formal oxidation states. Moreover,

the separation in potential, ΔE_0 in eq 1, for each polymer is small enough that there is substantial tervalent character to the formal zerovalent form. Before considering how these zerovalent materials can be formed, a few more theoretical and practical points are worthy of consideration. First, there are certain ways in which these neutraly charged tervalent materials are conceptually analogous to intrinsic semiconductors. The HOMO of the redox sites is analogous to the valence band, and the LUMO, to the conduction band. The HOMO−LUMO energy separation, which again is ΔE_0 as defined in eq 1, is the analog of the band gap. The 1+ and 1− sites are, respectively, analogous to thermally generated holes and electrons. A major difference is that the HOMOs and LUMOs of redox sites in these $[Ru(LL)_3]^n$-based polymers are highly localized; in semiconductor parlance this would correspond to very narrow bandwidths with relatively immobile charge carriers. At the same time, the band gap analog ΔE_0 is small; therefore, the relatively low charge carrier mobility is largely offset by the fact that the charge carrier concentrations are approaching 0.1 M at room temperature.

As with any electron-hopping polymer, electron transport in **P1**−**P3** is an activated process (vide infra). In any mixed-valent polymers containing electroinactive counterions, a majority of that activation energy can come from the need for local motions of these counterions. For the zerovalent form of these polymers both 1+ and 1− sites are mobile by electron hopping. Experimentally, the absolute conductivities of these polymers are much larger when $n = 0$ than when it has any other value.[22]

Finally, like an intrinsic semiconductor, the Fermi level energy of the zerovalent polymer should lie in the middle of the "band gap." That energy is defined for the polymers as $E_{(0,max)}$ in eq 2. The redox processes which produce the formal 1+, 0, and 1− oxidation states (and thus define $E_{(0,max)}$) are largely ligand-based processes. The potentials of those processes are therefore superbly sensitive to substitutions on the bipyridine rings. As a consequence, there is a huge capacity to tune those potentials, and thus the work function, by synthetic means. Ideally then, a monomer can be designed to produce a polymer with an a priori determined work function. Moreover, in general the potentials of the relevant redox processes are such that the conducting polymers would have relatively low work functions, in the 2.5−4.0 eV range.

Preparation of the Zerovalent polymer. In principle it should be straightforward to electrochemically convert a poly-$[Ru(LL)_3]^{2+}$ film into its zerovalent form; in practice it is less so. Under typical electrochemical conditions, there is a single potential where n will be precisely zero. Accurately predicting this potential would require that both the 1+/0 and 0/1− redox processes be ideal. Furthermore, even if this potential could be identified, there is no certainty that the film would truly be free of redox-inactive ions. When $n = 0$ there is no *requirement* that counterions be incorporated to balance charge; however, there is also no requirement that the polymer be free of ions as long as the cation and anion concentrations are equal. Each of these problems can be avoided by employing an electrolyte solution in which the cation is polymeric.[22]

In earlier work, we showed that poly(diallyldimethylammonium hexafluorophosphate), PDDA$^+$PF$_6^-$, can be used as a supporting electrolyte. The very large PDDA$^+$ cation is completely sterically blocked from entering each of the polymers considered here; consequently, the films cannot be reduced beyond the $n = 0$ form because there are no cations in solution which can enter the film to maintain charge neutrality. Moreover,
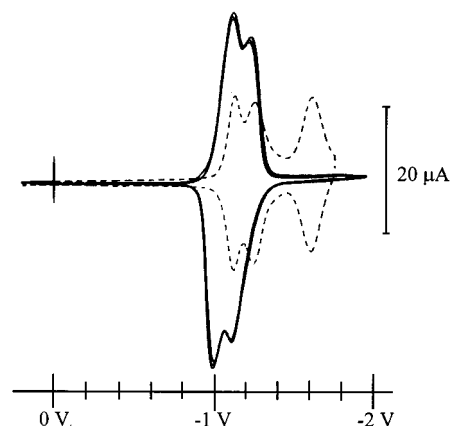

Figure 5. Cyclic voltammetry on **P2** films, in different electrolyte solutions. Dashed line is for a film in TBA$^+$PF$_6^-$ solution in CH$_3$CN, solid line a film in PDDA$^+$PF$_6^-$ solution. (WE) glassy carbon, (RE) Ag/Ag$^+$ 0.1 M in DMSO, (CE) Pt foil. The difference in the peak currents is due only to the fact that the films were of different thicknesses.

if cations cannot enter the film, it follows that the film cannot contain anions either (i.e., no salt). For this reason, cyclic voltammetry on the polymer films in a PDDA$^+$PF$_6^-$ electrolyte solution reveals only two possible reduction processes. Cyclic voltammetry on **P2** films in electrolyte solutions of PDDA$^+$PF$_6^-$ and TBA$^+$PF$_6^-$, where TBA$^+$ is the relatively small tetrabutylammonium cation, are shown in Figure 5. It is readily apparent that in the case of the polymeric electrolyte the third and subsequent reductions are blocked.

Films of **P1**−**P3** electrochemically reduced in a solution of PDDA$^+$PF$_6^-$ well past $E_0(0/1-)$ will indeed have been stripped of all counteranions and will be in the $n = 0$ state, as described above. At that point, the applied potential can be removed, and the film will remain in this state, provided that it does not encounter oxidizing agents. Resistivities of such films are on the order of 10^3 $\Omega\cdot$cm and do display a semiconductor-like temperature dependence as expected of a thermally activated electron-hopping process.[23]

IV. Results and Discussion

Fermi Energies. Thin polymer films were prepared on electrode surfaces from **M1**, **M2**, and **M3** (Figures 1, 2, and 3, respectively) as described in the Experimental Section. Electrochemical data obtained from these films are presented in Table 1, along with solution data from each of the three monomers in the same electrolyte (a TBA$^+$PF$_6^-$ acetonitrile solution). Fermi levels (E_F) were calculated from each set of data as the average of the $E_{1/2}$ of the second and third reductions. The use of either electrochemical data set for calculating E_F requires some caution. The solution data cannot account for any environmental or chemical effects on $E_{1/2}$ introduced by the polymerization process. The polymer data, on the other hand, is complicated by both steric effects and Donnan potentials effects on the $E_{1/2}$'s.[24] Since the problems associated with the polymer data are dependent on both the composition and concentration of the electrolyte and because it is not clear how one might quantitatively deconvolute these effects from the data, the solution results probably more accurately reflect redox values

(22) Elliott, C. M.; Redepenning, J. G.; Balk, E. M. *J. Electroanal. Chem.* **1986**, *213*, 203−215.

(23) Elliott, C. M.; Redepenning, J. G.; Balk, E. M.; Schmittle, S. J. *Electronically Conducting Films of Poly(trisbipyridine)-Metal Complexes;* ACS Symposium Series 360 (Inorganic and Organometallic Polymers); American Chemical Society: Washington, DC, 1988; pp 420−429.

(24) Naegeli, R.; Redepenning, J.; Anson, F. C. *J. Phys. Chem.* **1986**, *90*, 6227−6232.

Table 1: All Cyclic Voltammetry was Performed in a Luggin Capillary Cell with a Glassy Carbon WE, Pt Wire CE, and RE as Stated in the Table[a]

	$E_{1/2}$ vs Ag/Ag$^+$ ref		$E_{1/2}$ vs NHE ref				
	$E_{1/2}$ 1+/0 (V)	$E_{1/2}$ 0/1− (V)	$E_{1/2}$ 1+/0 (V)	$E_{1/2}$ 0/1− (V)	E_F calcd (V)	Φ, calcd (eV)	Φ, UPS (eV)
P1 film	−1.02	−1.32	−0.61	−0.91	−0.76	3.84	3.6
P2 film	−1.26	−1.61	−0.85	−1.20	−1.03	3.57	3.5
P3 film	−1.85	−2.00	−1.44	−1.59	−1.52	3.08	3.0
M1 monomer solution	−1.11	−1.27	−0.70	−0.86	−0.78	3.82	
M2 monomer solution	−1.35	−1.58	−0.94	−1.17	−1.06	3.54	
M3 monomer solution	−1.92	−2.15	−1.51	−1.74	−1.63	2.97	

[a] The electrolyte was 0.1 M TBA$^+$PF$_6^-$ in CH$_3$CN. E_F is reported vs an NHE electrode and work functions vs vacuum electron energy.

relevant to the calculation of E_F. Despite these caveats, the values of E_F calculated from both sets of data and displayed in Table 1 are in very close agreement with each other for all three polymers. That agreement suggests that the various perturbations on the redox processes considered above are, in the final analysis, fairly minor.

From these calculated E_F values, approximate work functions (Φ) are available. The energy required to remove an electron from the Fermi level to the vacuum energy level, which is approximately −4.60 eV versus normal hydrogen electrode (NHE) in the electrochemical potential scale,[25] is defined as Φ. Work functions can thus be taken as the difference between −4.60 eV and the calculated E_F. The work function of a conductor can be determined directly using ultraviolet photoelectron spectroscopy (UPS). In this case Φ is the difference in energy between the secondary photoelectron edge and the incident photons. Prior to UPS analysis, each polymer film was electrochemically reduced in an inert atmosphere glovebox, thoroughly rinsed with pure solvent, and transported into the ultrahigh vacuum system without contacting ambient air (as described in the Experimental Section). Results of UPS experiments are also tabulated in Table 1. The spectrally determined values of Φ are all quite close to the values predicted from the electrochemical data, a result which validates our premise that electrochemistry can reliably be used to predict work functions of these zerovalent polymers. Furthermore, since we know how to synthetically tune the redox properties of the monomer, it follows that it should be possible to predetermine the work function of a corresponding reduced polymer film.

Full UPS spectra for all three polymers, analyzing for both HeI and HeII source lines, can be found in the Supporting Information. To demonstrate the determination of work function from UPS, Figure 6 is a blowup of the high binding energy region for a HeI spectrum of a reduced **P3** film. A line fit to the secondary electron edge is shown, with the 0.1 eV subtraction in HBEC due to broadening[13] included (see Experimental Section). Again, the work function for a given film is determined by comparing this final HBEC value to the incident photon energy of 21.22 eV. To check for any effects due to interaction of the films with the platinum substrate, photoelectron spectroscopy was also performed on reduced **P2** films coated on highly ordered pyrolytic graphite (HOPG). Both work functions and valence structures from the films on HOPG substrates agree well with those on platinum.

Zerovalent P3 as an OLED Cathode. The work function of the reduced **P3** polymer is approximately 3.0 eV. Consequently, like calcium with Φ = 2.9 eV, it should be capable of injecting electrons into the conduction band of several common EL materials. In an effort to verify this assumption, first-generation OLED devices using Alq$_3$ as the EL material were constructed, replacing the traditional metal cathode with the

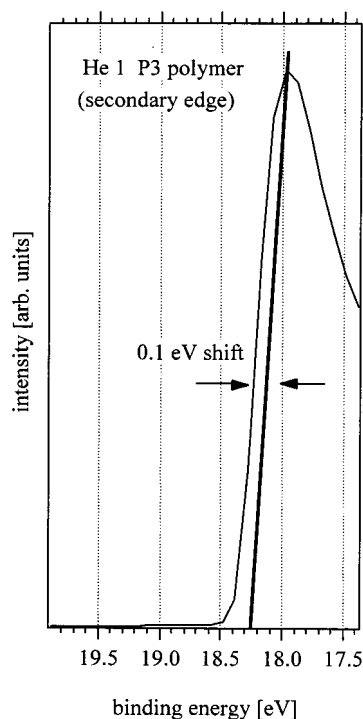(25) Trasatti, S. *Pure Appl. Chem.* **1986**, *58*, 955−966.

Figure 6. Determination of film work function. The HBEC is subtracted from the source energy, 21.22 eV.

electrochemically treated **P3** polymer. The **M3** monomer was spin-coated on a patterned ITO substrate, thermally polymerized, and electrochemically reduced all in a N$_2$ glovebox. Successive layers of Alq$_3$, TPD, and gold were thermally deposited in a vacuum chamber coupled to the glovebox. The layers were thus as follows: ITO substrate/reduced **P3** polymer cathode/Alq$_3$/TPD/Au anode (see Experimental Section for details). To electrochemically reduce the polymer prior to the addition of other layers, the **P3** cathode material must be deposited on a conductive surface. For this purpose, ITO serves quite adequately and is optically transparent. The reduced polymer itself has several intense absorption bands across the visible region of the spectrum; however, at the thickness employed the polymer is almost completely transparent—imparting only a barely perceptible purplish tinge to the ITO. Since this cathode is transparent, it is possible to construct these OLEDs with the anode on top and the light escaping through the cathode, which is an inverted arrangement relative to most devices in the literature. A few OLEDs with an inverted construction have been reported previously. In those cases a metal cathode was first deposited on a silicon substrate, followed by the organic layers and finally a transparent ITO anode.[14] Also, an ITO/Copper phthalocyanine layer has previously been reported as a transparent cathode material.[26]

The performance of OLEDs constructed with a **P3** cathode has thus far varied from one device to another, with a relatively
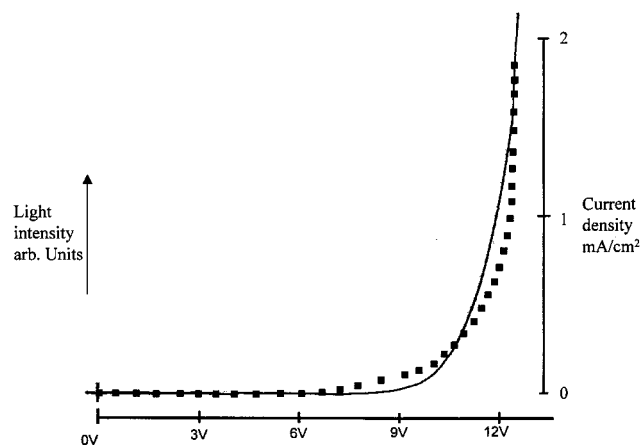
Figure 7. Current density vs voltage for a representative Alq_3-based OLED (dotted line, right-hand *y* axis). Light output vs voltage for the same device (solid line, left-hand *y* axis).

high incidence of electrical shorting. This problem was not unexpected and is almost certainly due, at least in part, to defects caused by particulate matter present in the lab and glovebox. Every effort has been taken to minimize the problem, and a fair percentage of the devices have performed as expected. At the same time, other defects such as pinholes are also possible sources of shorting. Current density versus voltage and light output versus voltage curves for a typical nonshorted device are shown in Figure 7. At approximately 9 V there is a sharp increase in current and light output. At this time calibrated light output data is not available, and the units for the light power are arbitrary. Qualitatively, however, the devices produce green-colored light that is easily visible to the naked eye at potentials at or above 10 V.

Again we emphasize that no serious efforts have yet been made to optimize the performance of these OLEDs. The shorting problems, we believe as stated above, are of known origin and should be greatly improved with better "clean-room" conditions. At the same time, the turn-on voltages and lifetime of these devices is sub-optimum. A suspected culprit in those regards is the hole-transport layer, TPD. Upon microscopic analysis, numerous devices have shown noticeable crystallization of the TPD layer. This is no doubt caused by heating or other damage upon thermal deposition of the adjacent gold layer. Indeed,

(26) Parthasarathy, G.; V. Khalfin, P. E. B.; Kozlov, V. G.; Forrest, S. R. *Appl. Phys. Lett.* **1998**, *72*, 2138−2140.

anode deposition on TPD has been shown to adversely affect device performance through this very mechanism.[14] The gold/TPD interface as such is likely problematic but was chosen for these devices due to equipment availability and expediency. Our present goal was simply to demonstrate that these new low work function polymers could serve as electron-injecting contacts. Preliminary work with other hole-transport/metal anode combinations strongly suggest that the problems extant with the present devices are soluble. Finally, the presence of the reduced **P3** film is essential to generating light in these devices. Identical devices constructed omitting the polymer layer have never been observed to produce light even with biases as large as 30 V.

V. Conclusions

Through this study we have demonstrated several things. First, it is possible to generate low work function conducting polymers which can serve as electron-injecting cathodes in OLEDs. Second, it is possible to tune the Fermi energies (and thus work functions) of these materials in predictable ways by synthetic modifications of the monomer. Finally, solution electrochemical data from the monomer can be used to predict the work function of the respective polymer with excellent accuracy.

As a consequence of the level of control one can exert over the electronic properties, in principle, polymeric cathodes can be tailored to match the band structure of each EL material. The availability of a series of different polymer cathode materials will provide an opportunity to study the EL material interface with polymers having very similar chemical compositions but varying work functions. Such fundamental studies should be relevant to important practical considerations in OLED operation such as stability, efficiency, and turn-on voltage.

Supporting Information Available: Additional figures (PDF). This material is available free of charge via the Internet at http://pubs.acs.org.

JA011333E